10-13-2012

Past and future wind climates over the contiguous USA based on the North American Regional Climate Change Assessment Program model suite

SC Pryor

RJ Barthelmie

Justin T. Schoof
Southern Illinois University Carbondale, jschoof@siu.edu

Recommended Citation
Pryor, SC, Barthelmie, RJ and Schoof, Justin T. "Past and future wind climates over the contiguous USA based on the North American Regional Climate Change Assessment Program model suite." *Journal of Geophysical Research* 117 (Oct 2012). doi:doi:10.1029/2012JD017449.

Past and future wind climates over the contiguous USA based on the North American Regional Climate Change Assessment Program model suite

S. C. Pryor,[1] R. J. Barthelmie,[1] and J. T. Schoof[2]

Received 6 January 2012; revised 5 September 2012; accepted 9 September 2012; published 13 October 2012.

[1] Multiple descriptors of wind climates over the contiguous USA from a suite of thirteen simulations conducted with five Regional Climate Models (RCMs) nested within reanalysis data and four Global Climate Models are evaluated relative to the North American Regional Reanalysis (NARR) and independent observations. Application of the RCMs improves 'forecasts' of wind climates during 1979–2000 relative to the driving reanalysis, and the RCMs exhibit some skill in depicting historical wind regimes. However, the relative paucity of reference data sets for wind climates represents a significant challenge to evaluation of the modeled wind climates. Simulation of intense and extreme wind speeds by the RCMs are, to some degree, independent of the lateral boundary conditions, and instead exhibit greater dependence on the RCM architecture. RCMs that do not employ a hydrostatic formulation have higher skill in manifesting the macro-scale variability of extreme (20 and 50 year return period) wind speeds even when the RCM are applied at the spatial resolution of 50 km. Output from RCM simulations conducted for the middle of the current century (2041–2062) indicate some evidence of lower intense wind speeds particularly in the western U.S., but no difference in extreme wind speeds, relative to 1979–2000.

Citation: Pryor, S. C., R. J. Barthelmie, and J. T. Schoof (2012), Past and future wind climates over the contiguous USA based on the North American Regional Climate Change Assessment Program model suite, *J. Geophys. Res.*, *117*, D19119, doi:10.1029/2012JD017449.

1. Introduction and Objectives

[2] Understanding how climate non-stationarity has been manifest as changes in near-surface wind regimes in the past and how near-surface wind speed regimes might alter in the future is of great value to a number of socio-economic sectors. For example, extreme wind speeds are used in design standards to ensure structural integrity under extreme loading cases [*Cook*, 1986] and high magnitude extreme wind speeds (and gusts) have been linked to failures in the electricity distribution network [*Banik et al.*, 2010; *Reed*, 2008], infrastructure damage and insurance losses [*Schwierz et al.*, 2010]. However, comparatively little research has explicitly assessed the skill of Regional Climate Models (RCMs) in simulating contemporary wind climates [*Kunz et al.*, 2010; *Pryor et al.*, 2012a, 2012b; *Winterfeldt et al.*, 2011]. Further, relatively few studies have used multimodel suites to assess the sensitivity of wind climates to the lateral boundary conditions and global climate non-stationarity. Thus the questions that motivate this research are threefold:

[3] 1. How skillful are the members of the North American Regional Climate Change Assessment Program (NARCCAP) RCM suite in reproducing the contemporary near-surface wind speed climate over North America? Does the degree of skill vary with wind speed metric (i.e., the distribution parameter under consideration)?

[4] Model performance in reproducing the historical climate is not per se indicative of skill in climate change detection and attribution [*Santer et al.*, 2009]. Previous analyses of climate model output have indicated only a weak relationship between 'skill' in reproducing features of the historical and contemporary climate and the magnitude of predicted change [*Knutti et al.*, 2010]. Nevertheless, information regarding model performance in the historical and contemporary climate is one way to assess the 'value added' by dynamical downscaling [*Castro et al.*, 2005; *Feser et al.*, 2011; *Winterfeldt et al.*, 2011]. Further, such assessments remain a useful component of climate change analyses to contextualize projected changes in geophysical parameters. They also provide a mechanism to at least partially evaluate the ability of models to simulate dynamical linkages responsible for inducing variability in the historical period. Accordingly, we present an evaluation of multiple aspects of the wind climates as simulated by the NARCCAP models relative to the NCEP-2 reanalysis [*Kanamitsu et al.*, 2002], the North

[1]Atmospheric Science Program, College of Arts and Sciences, Indiana University, Bloomington, Indiana, USA.
[2]Department of Geography and Environmental Resources, Southern Illinois University, Carbondale, Illinois, USA.

Corresponding author: S. C. Pryor, Atmospheric Science Program, College of Arts and Sciences, Indiana University, 702 N. Walnut Grove, Bloomington, IN 47405, USA. (spryor@indiana.edu)

0148-0227/12/2012JD017449

American Regional Reanalysis (NARR) [*Mesinger et al.*, 2006] and observational data sets. NARR was selected a priori as the primary reanalysis product against which to evaluate the NARCCAP simulations because it is the reanalysis product with the highest spatial and temporal resolution over the contiguous USA and because NARR uses NCEP-2 reanalysis to provide the lateral boundary conditions thus enabling direct comparison with the NCEP-2 nested RCM simulations. However, as described below, we also use other observationally derived data sets to provide additional evaluation of the RCM output.

[5] 2. How sensitive are varying metrics of the modeled near-surface wind speed climate to the lateral boundary conditions versus variations in RCM applied?

[6] There are multiple sources of uncertainty in downscaled climate projections including (but not limited to); those deriving from the architecture of the model used to provide the lateral boundary conditions and/or predictors for empirical downscaling, the architecture of the (empirical or dynamical) downscaling model, initial conditions (and internal climate variability), and the radiative forcing. Understanding the magnitude and origin of these uncertainties provides a mechanism for potentially enhancing and improving climate projections [*Hawkins and Sutton*, 2009]. In prior probabilistic downscaling of wind climates over Northern Europe, the coupled Atmosphere-Ocean Global Climate Model (AOGCM) used to provide the downscaling predictors was found to dominate uncertainty in downscaled 90th percentile wind speeds for the end of twenty-first century. Variations in initial conditions and radiative forcing make lesser (but non-negligible) contributions to the projection uncertainty [*Pryor and Schoof*, 2010]. Dynamical downscaling analyses of projected changes in extreme wind climates and lower moments of the wind speed distribution over Northern Europe also exhibited a high degree of dependence on the lateral boundary conditions (AOGCM). The RCM applied additionally had a substantial impact on the magnitude and direction of change in wind speed metrics. Internal variability and initial conditions exert a stronger impact on projected extreme wind climates throughout the twenty-first century than is manifest in measures of the wind speed central tendency [*Pryor et al.*, 2005; *Pryor et al.*, 2012a]. The dominance of AOGCM architecture as a source of uncertainty in climate projections over northern Europe is consistent with a priori expectations since, for example, the surface conditions used within RCM are typically held constant. Lateral boundary conditions were also found to be the leading source of uncertainty in climate projections in analyses of thermal [*Rowell*, 2006] and hydrological [*Kay et al.*, 2009] regimes. Here we compare the sensitivity of wind climates from the NARCCAP simulations in 1979–2000 to variations in the lateral boundary conditions and the RCM applied.

[7] 3. What do the simulations from the NARCCAP model suite imply about possible changes in the near-surface wind climate over North America?

[8] Within the midlatitudes the dynamical linkages between a warming climate and the near-surface winds are complex [*O'Gorman*, 2010]. In regions where the atmospheric flow is not dominated by thermo-topographic effects, the wind climate is principally determined by transitory synoptic-scale anticyclone and cyclones [*Weisse and von Storch*, 2010]. Cyclone development is a baroclinic process, and thus it is relatively insensitive to equator to pole temperature gradients, since it is a function of smaller-scale variance of the temperature field. Thus it may be more strongly influenced by the likely increase in upper tropospheric thermal gradients than possible decreases in near-surface temperature gradients [*Held*, 1993]. The coupling between scales is reciprocal. These 'storm track' cyclones and anticyclones are both steered by the larger-scale flow and help to reinforce it [*Woollings*, 2010]. While steering of transitory synoptic scale systems is also influenced by the large-scale thermal gradient, this link is also indirect. There may be a strong influence of higher water-holding capacity and energy availability due to the phase transfer of water [*Chang et al.*, 2002]. Additionally, the link between the upper-level flow fields and near-surface wind speeds is strongly mediated by factors such as atmospheric stability and land cover that influence momentum transfer from aloft.

[9] In contrast to other geophysical variables, analyses designed to quantify historical evolution of wind climates exhibit highly divergent results depending on the precise data period considered and the data record analyzed. This may be due in part to the complexities of dynamical linkages described above. It may also be symptomatic of the lack of robust, long-term and homogenized data sets for wind speeds. Analysis of output from historical data sets, reanalysis products and two RCMs found no consistency with respect to historical tendencies of wind climates over the contiguous U.S. in the latter part of the twentieth century (1973–2005) [*Pryor et al.*, 2009]. The observational data sets generally indicate declines in both the 50th and 90th percentile wind speeds over the eastern USA, while converse trends are seen in output from NARR, global reanalysis data sets and simulations using the Regional Spectral Model nested in NCEP-2 [*Pryor et al.*, 2009].

[10] The majority of prior research to develop wind climate projections has tended to focus on mean wind speeds and has indicated only modest changes in wind climates over the USA. Analysis of direct output from previous generation Canadian Climate Center and Hadley Center General Circulation Models (GCMs) indicates reduced multiyear annual mean wind speeds over North America in projections for the twenty-first century, but the mean wind speed will likely remain within ±5% of historical values (and thus within the envelope of current inter-annual variability) [*Breslow and Sailor*, 2002]. Empirical downscaling of four CMIP-3 generation GCMs indicated summertime wind speeds in the Pacific Northwest may decrease by 5–10%, while wintertime wind speeds remained very close to current values [*Sailor et al.*, 2008]. High resolution modeling over California and Nevada with the Weather Research and Forecasting (WRF) model (applied at 4 km) nested within the Parallel Climate Model (PCM) AOGCM for 2047–2056 and 1997–2006 found no change in the probability distribution of daily wind speeds in the climate projection period relative to the contemporary climate in either summer or winter [*Pan et al.*, 2011]. Small increases in projected wind speeds over the next 30 years were detected in dynamical downscaling analysis of PCM over the Caribbean [*Angeles et al.*, 2010]. Prior analyses of a suite of four AOGCM-RCM couplings from the NARCCAP project indicate average annual mean energy density in 2041–2062 for all grid cells over the contiguous USA is within ±25% of historical values

Lateral boundary conditions (AOGCM) → RCM↓	NCEP-2	CGCM3	CCSM	GFDL	HadCM3
CRCM (Non-hydrostatic, spectral nudging, 900 sec)	1979-2000 ●	1979-2000 □ 2041-2062	1979-2000 ◊ 2041-2062		
HadRM3 (Hydrostatic, 900 sec)	1979-2000 ●				1979-2000 □ 2041-2062
MM5I (Non-hydrostatic, 120 sec)	1979-2000 ●		1979-2000 □ 2041-2062		
RegCM3 (Hydrostatic, 300 sec)	1979-2000 ●	1979-2000 □ 2041-2062		1979-2000 ◊ 2041-2062	
WRFG (Non-hydrostatic, 150 sec)	1979-2000 ●	1979-2000 □ 2041-2062	1979-2000 ◊ 2041-2062		

Figure 1. Matrix of coupled Atmosphere-ocean General Circulation Model (AOGCM, or NCEP reanalysis) and Regional Climate Model (RCM) simulations used here. NCEP-2 denotes the NCEP-DoE reanalysis data [*Kanamitsu et al.*, 2002]. The AOGCMs are: GFDL = Geophysical Fluid Dynamics Laboratory model (CM2.1) [*Delworth et al.*, 2006], CGCM3 = Canadian model [*Scinocca et al.*, 2008], HadCM3 = Hadley Centre model [*Pope et al.*, 2000], CCSM = Community Climate System Model version 3 [*Collins et al.*, 2006]. The RCMs are: RegCM3 = Regional Climate Model 3 used by UC-Santa Cruz [*Pal et al.*, 2007], CRCM = Canadian Regional Climate Model [*Elía and Côté*, 2010], HRM3 = Third generation Hadley Centre RCM [*Jones et al.*, 2004], WRFG = Weather Research and Forecasting model (with the Grell cumulus parameterization) [*Skamarock et al.*, 2005], MM5I = Pennsylvania State University/National Center for Atmospheric Research mesoscale model (version 5) [*Grell et al.*, 1995]. The application of spectral nudging, the hydrostatic/non-hydrostatic formulation and time step used in each RCM simulation is noted in parentheses in the first column. The values in the grid cells indicate the availability of model output for each AOGCM-RCM coupling for each period. The symbols shown in the figure depict those used in Figures 4 and 5 in comparison of the simulations from the historical period relative to NARR, and in Figure 7 for comparison with extreme wind speeds from station observations.

(1979–2000) for all model simulations [*Pryor and Barthelmie*, 2011]. Here we draw from a wider array of AOGCM-RCM couplings and examine a more extensive array of metrics of the wind climate over North America for the middle of the current century relative to those same metrics computed for the end of the twentieth century to examine whether, and where, there is evidence of a possible shift in wind climates, and how consistent any projected changes are across the model suite.

2. Data and Methods Used

[11] The RCM simulation output analyzed herein is drawn from the North American Regional Climate Change Assessment Program (NARCCAP) (see Figure 1 for a summary of the simulations used) [*Mearns et al.*, 2009]. The NARCCAP program was designed to conduct a comprehensive suite of RCM simulations necessary to systematically investigate uncertainties in regional scale projections of future climate over North America and generate climate change scenarios for use in impacts research. A suite of RCMs were nested within lateral boundary conditions from both 'observed' reanalysis data (NCEP-2) [*Kanamitsu et al.*, 2002], and a series of AOGCMs for a historical period and for a time slice of the middle twenty-first century. The RCM were run at a resolution of 50 × 50 km, and the wind components at a nominal height of 10 m a.g.l. were archived at a temporal resolution of 3 h. The future simulations are for the A2 emissions scenario which equates to global greenhouse gas emissions of approximately 80 Gt carbon dioxide equivalents (CO_2-eq) per year (twice the emissions of 2000) by approximately 2055 [*Nakicenovic and Swart*, 2000]. However,

given the future period considered is relatively near-term, variations in climate states between different radiative forcing scenarios is comparatively modest [*Intergovernmental Panel on Climate Change*, 2007]. Hence results presented herein are likely representative of the majority of possible emission trajectories and thus climate forcing. The climate sensitivity of the AOGCMs ranges from 2.7 to 3.4°C (with CCSM showing the lowest global temperature response to doubling of CO_2 and the other three AOGCMs showing a response of either 3.3 or 3.4°C) [*Mearns et al.*, 2009].

[12] It has been suggested that the damage function of climate change is likely to be strongly influenced by the occurrence of low-probability, but high-impact, outcomes [*Weitzman*, 2011]. Given the importance of metrics beyond the central tendency to the impacts of climate change, we use a range of metrics to evaluate the NARCCAP suite of simulations and expand consideration beyond the ability to capture the mean climatological state. Percentile values of the wind speed distribution for any given RCM grid are derived from rank ordering of model output. We estimate the 20- and 50-year return period wind speed by fitting of annual maxima from each simulated or observational time series to a double exponential cumulative probability distribution, and computing the return period wind speed from:

$$U_T = \frac{-1}{\alpha} \ln\left[\ln\left(\frac{T}{T-1}\right)\right] + \beta \quad (1)$$

where: U_T is the wind speed for a given return period ($T = 20$ or 50 years) and the distribution parameters (α and β) are derived from the mean and variance of the time series of annual maximum values [*Abild et al.*, 1992].

[13] Time series of near-surface wind measurements from in situ stations are subject to inhomogeneities [*Pryor et al.*, 2009] and reflect conditions at spatial scales far below those that characterize RCM output [*Garratt*, 1992]. Thus the primary data set used to provide the observational data against which the RCM simulations are compared is the North American Regional Reanalysis (NARR) [*Mesinger et al.*, 2006]. NARR wind speeds are archived with a 3-hourly time step (equal to that of the NARCCAP simulations) and an output grid resolution of approximately 32 × 32 km, which is slightly higher spatial discretization than the NARCCAP RCM suite. The lateral boundary conditions from NARR are drawn from NCEP-2 and thus are consistent with some of those used for the 'observationally' driven NARCCAP RCM simulations. We conduct an analysis in which NARR is used as the 'target' and the NCEP-2 wind fields as a 'reference' forecast against which we compare the RCM output. This analysis thus indicates the degree of "added value" in applying the RCMs.

[14] In addition to the NARR data set we also examine extreme wind speeds derived from the RCM output compared to those obtained via extrapolation of daily maximum observed (fastest mile) wind speeds at 35 stations contained in the National Institute of Standards and Technology (NIST) extreme wind data archive (www.itl.nist.gov/div898/winds/daily.htm). The station observations from NIST originated from the National Climate Data Center (NCDC) and were collected at stations located in open terrain at a typical height of approximately 6 m. These data were extrapolated to a nominal height of 10 m a.g.l. using the logarithmic wind profile and a roughness length of 0.05 m prior to being archived by NIST. These data were transformed from one-minute into 10-min sustained wind speeds using a scaling factor 0.855 [*Simiu and Scanlan*, 1978], prior to determining the annual maxima and calculation of the extreme wind speeds at each station. This scaling factor is also cited within the ASCE Manual 'Guidelines for electrical transmission line structural loading' (3rd edition) as suitable for well-exposed sites such as those in the NIST database. However, it should be noted that prior work provides evidence that sites in different climatological regimes (e.g., in tropical cyclone prone areas, or in regions with strong topographic forcing) may exhibit differential scaling with wind speed averaging period. The observations derive from 1965 to 1990 and are not subject to major discontinuities introduced by the transition to the ASOS system (starting in the early 1990s). However, the time period of the data records is partially offset from the RCM simulations. Only years in which a given station has more than 99% of observed fastest mile wind speeds present were used to compute annual maximum wind speeds for estimating extreme wind speeds. For all 35 stations over 15 years of data pass this threshold.

[15] We also evaluate NARCCAP output in terms of the ability of the RCMs to reproduce the spatial variability of the energy density in the wind ($E = 0.5\rho U^3$, where ρ is the air density and U is wind speed), using data from the National Renewable Energy Laboratory's (NREL) assessment of the wind energy density over the contiguous USA [*Elliott et al.*, 1986]. In this analysis the time series of wind speeds in each grid cell of the RCM simulations of 1979–2000 were multiplied by 1.258 to scale from a nominal height of 10-m to 50-m a.g.l. [*Pryor and Barthelmie*, 2011] and used to compute an average energy density in each grid cell for comparison with grid cell categorical estimates of E from the NREL wind power assessment (shown in Figure 2) [*Elliott et al.*, 1986].

[16] Given that the scales at which regional climate modeling 'adds value' are likely to be coarser than the dimensions of individual grid cells [*Feser et al.*, 2011; *Laprise*, 2003], while we present some analyses of output from individual grid cells, we also evaluate the model output integrated over larger spatial scales. In these syntheses model performance and climate projections are aggregated in six regions that broadly represent those used in the National Climate Assessment and that were used previously in *Pryor and Barthelmie* [2011] (see Figure 2).

[17] Wind speeds in the midlatitudes exhibit a high degree of both inter-annual and intraannual variability [*Bärring and Fortuniak*, 2009; *Weisse and von Storch*, 2010; *Pryor and Ledolter*, 2010].Thus, the inter-annual and intraannual variability of mean wind speeds for the contemporary climate in each of the six regions shown in Figure 2 is also presented for the NARR data set and each of the NCEP-RCM and AOGCM-RCM couplings for 1979–2000. The variability is characterized as the spatially averaged ratio of the grid-cell specific standard deviation of mean wind speed (computed across the seasonal cycle or across the years) to the mean wind speed in that grid cell.

[18] The time period used for the analyses of the contemporary climate is 1979–2000 since it is the longest common period for which all RCM simulations are available. An exception is that the CCSM-driven runs end in 1999, thus

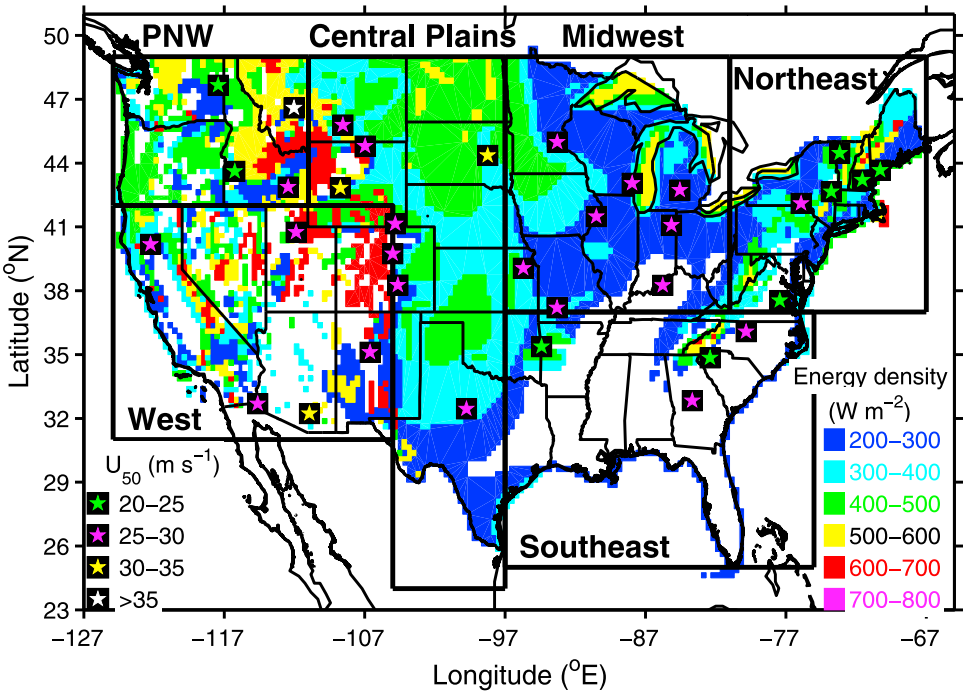

Figure 2. Spatial domain of the analyses presented herein. The colors denote the annual average wind resource (expressed as an energy density in W m^{-2}) at 50 m from a data driven assessment conducted by the National Renewable Energy Laboratory (NREL) [*Elliott et al.*, 1986]. The six regions shown are used in regional analyses presented in Figures 5, 7, 9 and 10. The regions are: Pacific Northwest (PNW), West (W), Central Plains (CP), Midwest (MW), Southeast (SE) and Northeast (NE). The solid black squares denote the locations from which fastest run wind speeds are used and the internal symbol indicates the 50-year return period wind speed derived from data collected at those stations.

for the CCSM nested RCM simulations the time series were resampled to generate a 22nd year (conserving the appropriate seasonality). For comparability, a 22 year future period (2041–2062) is selected for the analysis of possible climate change signals.

[19] We use six primary statistical metrics to depict the degree of agreement between modeled and reanalysis/observational data sets; the Pearson and Spearman correlation coefficients (r), the root mean square difference (RMSD), the mean bias (⟨Bias⟩), the t-test for difference of means, and the Brier skill score (BSS). The BSS is computed using the decomposition of *Murphy and Epstein* [1989] as presented in *von Storch and Zwiers* [1999]:

$$BSS = \frac{\rho^2_{F'P'} - \left(\rho_{F'P'} - \frac{\sigma_{F'}}{\sigma_{P'}}\right)^2 - \left(\frac{\langle P'\rangle - \langle F'\rangle}{\sigma_{P'}}\right) + \left(\frac{\langle P'\rangle}{\sigma_{P'}}\right)^2}{1 + \left(\frac{\langle P'\rangle}{\sigma_{P'}}\right)^2} \quad (2)$$

where:

[20] F the 'forecast', i.e., wind speeds from RCMs nested in the NCEP-2 (or AOGCM) lateral boundary conditions;

[21] P the 'reference' (NARR) wind climate;

[22] F′ the difference between the 'forecast' from a RCM and NCEP-2;

[23] P′ the difference between NARR and the reference NCEP-2.

[24] The BSS therefore quantifies the 'added value' of the RCMs [*Winterfeldt et al.*, 2011] in terms of the simulation of near-surface wind speeds in the historical period (1979–2000).

[25] To calculate the BSS, the spatial fields of each wind speed metric from NCEP-2, NARR and the RCMs were interpolated to a common 0.5 × 0.5° grid using a standard point kriging algorithm. To avoid issues introduced by interpolation of spatial fields with widely differing resolution or direct comparison of grid cells that have comparatively little common area, in the other analyses time series of wind speeds in a given RCM grid cell are compared with NARR time series from the nearest grid cell *only* if the RCM grid cell centroid lies within 19 km of the NARR centroid. Use of this distance threshold ensures >60% of the NARR grid cell lies within the RCM grid cell. For the analysis of the consistency of the climate change signal across RCM-AOGCM coupling, a grid cell is only considered if *all* RCMs have a grid cell centroid with 19 km of the NARR grid cell center. In analyses of regionally integrated data output from each of the RCMs are maintained on their original grid, and the selection criteria is that the center of the model grid cell must lie within the bounds of the region (where the regions are as shown in Figure 2).

3. Results

3.1. Model Skill in the Historical Period Relative to NARR and Observations

[26] All of the RCM simulations nested in NCEP-2 exhibit higher spatial variability over the study domain than is

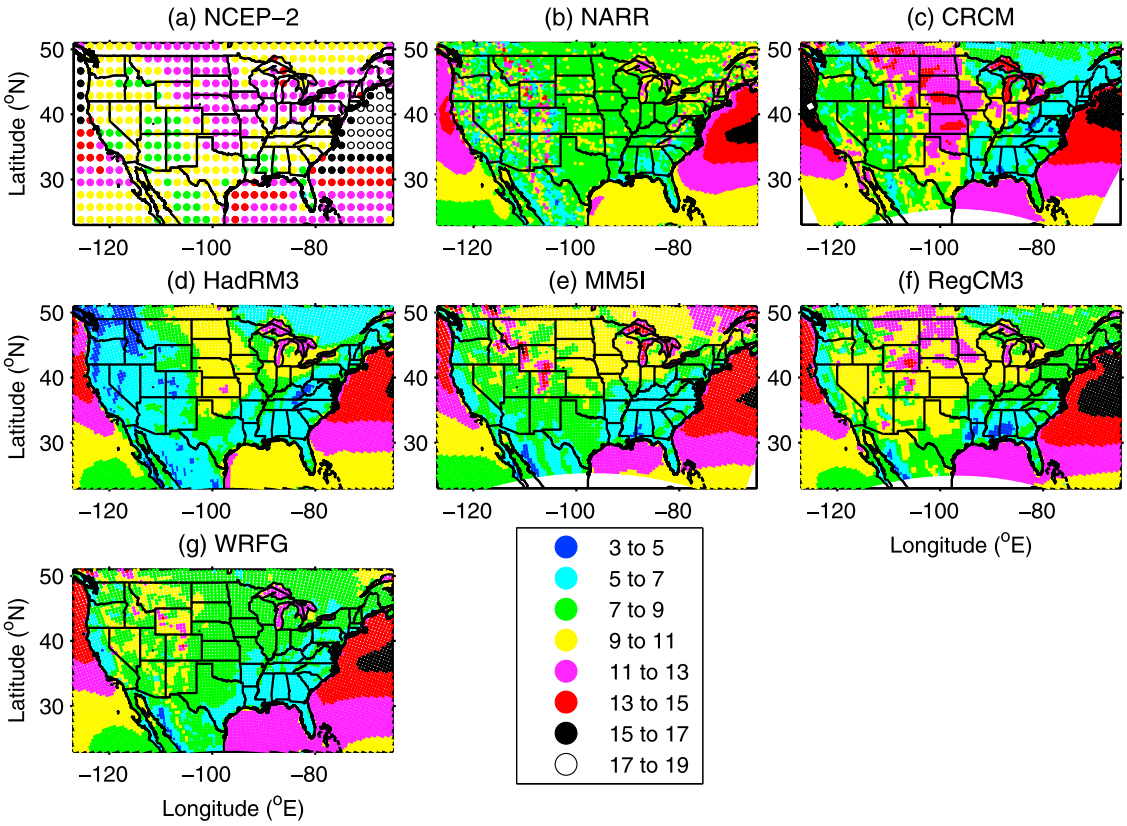

Figure 3. Spatial fields of the mean annual 95th percentile wind speeds (m s^{-1}) for 1979–2000 from (a) NCEP-2, (b) NARR, (c) CRCM, (d) HadRM3, (e) MM5I, (f) RegCM3, and (g) WRFG. Simulations for Figures 3c–3g are for simulations nested within NCEP-2.

manifest in output from NARR for all of the wind speed distribution descriptors (see Figures 3 and 4). This is partly due to the fact that the RCM simulations exhibit higher values in the Central Plains than is evident in the NARR output. The Central Plains region exhibits both high wind energy resource magnitudes (Figure 2) and penetration of electricity generation from that source (see map of wind energy deployments as of the end of 2010 provided in *Pryor and Barthelmie* [2011]). This region does not exhibit comparable enhancement of wind speeds in NARR to those manifest in wind resource assessments (Figure 2 and *Lu et al.* [2009]), the NCEP-2 data set or the RCM output (e.g., Figure 3). As indicated by the BSS decomposition, this appears to indicate a weakness in the NARR data set.

[27] The mean spatial fields for all wind speed metrics and all AOGCM-RCM combinations exhibit Pearson correlation coefficients (r) > 0.4, and all those for NCEP-2 nesting exceed 0.5 indicating some commonality in the spatial variability of the wind climate (Figure 4). Consistent with the example given in Figure 3, the spatial variability is uniformly higher in the RCM simulated fields than in NARR for all six wind speed metrics (i.e., $\sigma_m/\sigma_r > 1$). The RMSD between spatial fields of the various wind metrics derived from NCEP-2 nested RCM simulations and NARR, appears to be slightly amplified as one considers increasingly extreme (or rare) events (Figure 4). There is also greater divergence in the spatial patterns of extreme wind speed values between the RCM simulations (as indicated by the greater dispersion of points in Figures 4e and 4f relative to Figure 4a). This is consistent with physical reasoning. While the central tendency of the wind speed distribution at a given site may be largely a function of its location relative to the storm track (and thus the midlatitude cyclones entering the domain from the AOGCM or NCEP-2), the intensification (or not) of those systems may be more strongly determined by the RCM.

[28] Prior to interpreting the terms in the BSS it is important to note that NARR is not independent of NCEP-2. NCEP-2 is used to provide the lateral boundary conditions for NARR and the reanalysis systems and assimilated data share many commonalities. Despite this, Figure 3 illustrates that the wind climates over the study region differ markedly between the NARR and NCEP-2 reanalyses. Specifically, the 95th percentile wind speed at 10-m above ground level is virtually uniformly higher in output from NCEP-2 than NARR. In the BSS F′ is the difference between the 'forecast' from an RCM at a given location and the 'reference' (NCEP-2) and P′ is the difference between NARR and the reference (NCEP-2). If the BSS is positive then the forecast (from the RCM) is a more accurate representation of the NARR wind climate than the reference forecast (NCEP-2). Thus the downscaling is 'adding value'. If the BSS is negative, then the accuracy of the forecast relative to NARR is lower than the reference (NCEP-2). The first term in equation (2) is referred to as a measure of 'potential' skill – it is the square of the spatial anomaly correlation coefficient and, in the NCEP-2 nested RCM fields considered herein, it is uniformly highest for the WRFG simulations (i.e., 0.25 to 0.46 for all six descriptors of the wind speed distribution). The second

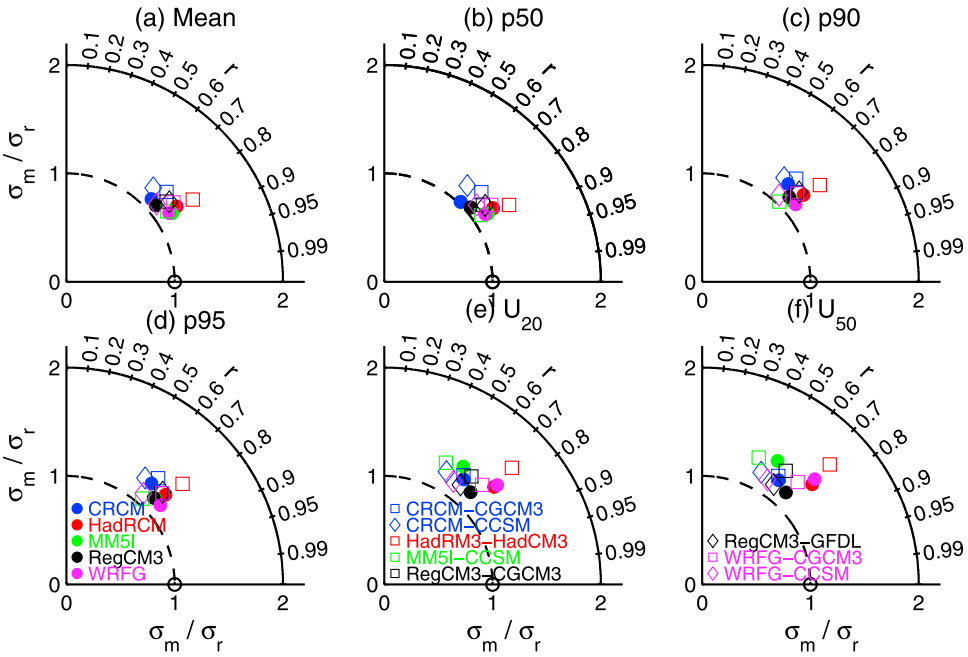

Figure 4. Taylor diagrams of the spatial fields of (a) Mean, (b) 50th percentile, (c) 90th percentile (d) 95th percentile, (e) 20-year return period and (f) 50-year return period wind speeds in simulations conducted with the specified RCM nested within NCEP-2 (solid symbols) and each of the AOGCMs (open symbols) versus fields computed from the NARR data set for 1979–2000. The statistics were computed only for RCM data points where the grid cell centroid is within 19 km of a centroid in NARR. The symbols used are as in Figure 1, and shown in Figures 4d–4f.

term is a measure of the conditional bias in the 'forecast' anomalies. It is the square of the difference between the anomaly correlation coefficient and the ratio of the standard deviation of the anomalies in the forecast fields (RCM output) and NARR (the 'reference forecast') relative to NCEP-2. This term is largest (and thus make a large negative contribution to relative skill) for CRCM simulations for the lower moments (mean and 50th percentile wind speeds), but is largest for MM5I for the extremes (20 and 50-year return period wind speeds). This implies that the relative conditional bias from the different RCMs differs by wind speed metric. The third term is a measure of the overall bias in the forecast anomalies. It is proportional to the difference in the mean anomaly from the forecast (RCM output) and the target (NARR) relative to NCEP-2 divided by the standard deviation of the anomalies in the target (NARR) relative to NCEP-2. This term is smallest (contributing to increased skill) for the CRCM simulations of the extreme wind speeds, and is smallest for the MM5I fields for the metrics of central tendency. The final term $\left(\frac{\langle P' \rangle}{\sigma_{P'}}\right)^2$ is an index of the degree of agreement between the target (NARR) and the reference (NCEP-2). It is the square of the ratio of the mean anomaly in the analyzed wind speeds (NCEP-2 to NARR) to the standard deviation of the anomalies. As the reference 'forecast' increases in skill, this term decreases in magnitude. However, in the analyses presented herein, this term is large (approximately 2–3), indicating that the NCEP-2 reanalysis output differs substantially in terms of the wind climate from the NARR (see the example given in Figure 3).

[29] The BSS for NCEP-2/RCM fields relative to NCEP-2 as a 'fit' to the NARR data set indicate that, with exception of the 50th percentile wind speed from the RegCM3 RCM, all of the NCEP-2 nested RCM simulations exhibit greater skill in representing the spatial variability in NARR than NCEP-2 (Figure 5a). This indicates that application of the RCMs is indeed 'adding value' although the BSS for individual RCM simulations exhibit considerable variability with the wind speed metric. For example, MM5I nested in NCEP-2 exhibits high skill scores for the lower moments of the wind speed probability distribution, but relatively low skill for the extremes (Figure 5a). Conversely, CRCM exhibits only very modest enhancement of skill over NCEP-2 for the lower moments but relatively high skill for the extreme metrics. This is also true for RegCM3. Consistent with visual inspection of Figure 3, WRFG exhibits the highest BSS for the 90th and 95th percentile wind speeds, indicating greatest 'forecast' improvement over NCEP-2 for these aspects of the wind climate.

[30] Only HadRM3 exhibits negative mean bias for the wind speed metrics relative to NARR. All other RCMs exhibit positive mean bias (i.e., higher wind speeds) for all of the metrics considered (Figure 5b). Consistent with the relatively low BSS for RegCM3 simulations of the mean and 50th percentile wind speed, the bias is highest for this RCM when nested in NCEP-2 for these measures of the central tendency (Figure 5b). The spatially averaged mean bias in the 20 and 50-year return period wind speeds is smallest for the CRCM simulations, but is relatively high for the extreme values derived from the MM5I simulation. The RMSD between spatial fields from the NCEP-2/RCM couplings

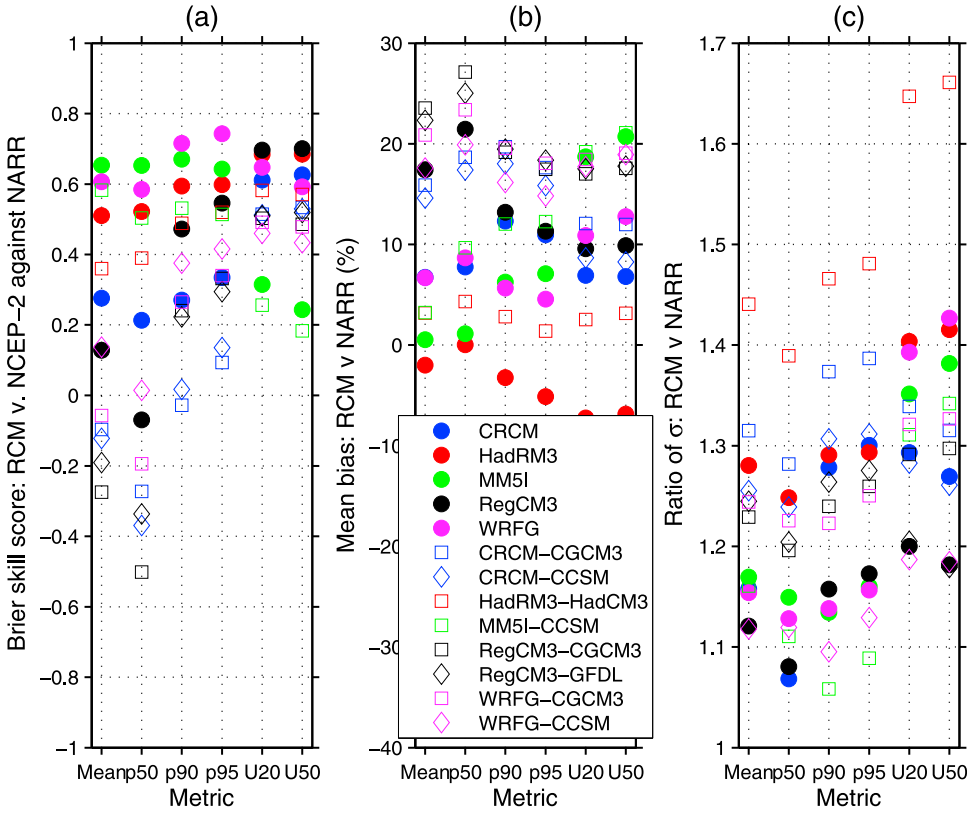

Figure 5. (a) Brier skill scores for the RCM simulations relative to NCEP-2 against NARR for the six wind speed distribution metrics. (b) Mean bias and (c) ratio of the standard deviation of fields from the RCM simulations relative to NARR. Note that for these comparative statistics the spatial fields from each data source were interpolated using a kriging algorithm onto a common 0.5 × 0.5° grid.

and NARR is largest for HadRM3 except for the 50-year return period wind speed, and is typically smallest for NCEP-2/RegCM3 simulations (Figure 5c).

[31] The three summary statistics for comparison of spatial fields of the six wind speed metrics presented in Figure 5 highlight three different aspects of RCM evaluation. Figure 5a, the BSS, emphasizes the added value of applying the RCMs and that the degree of value added is a strong function both of the specific RCM and the metric under consideration. While virtually all RCMs exhibit positive skill scores, no RCM performs 'best' according to the BSS for all wind speed metrics. Further, there is no clear evidence that the added value is increased (or decreased) in any specific aspect of the probability distribution. The former emphasizes the value of multimodel analyses, while the latter indicates that the RCM are not exhibiting substantially higher value in describing the spatial variability of mean wind speeds relative to the right tail of the probability distribution. Figure 5b re-emphasizes the positive bias of four of the five RCMs relative to NARR when the lateral boundary conditions are provided by NCEP-2. Indeed, as shown in Figure 3, NARR is also negatively biased relative to wind speeds from NCEP-2 (cf. Figure 3a versus Figure 3b). Figure 5c shows the ratio of the spatial variability (described using the spatial standard deviation) between RCMs and NARR. This ratio of standard deviation exceeds 1 for all of the RCM simulations indicating that the spatial fields from the RCM simulations exhibit considerably more spatial variability than is manifest in NARR. This taken in conjunction with other evidence presented herein, may indicate the NARR data set under-estimates both the magnitude of wind speeds and the spatial variability in wind climates over the contiguous USA.

[32] Virtually all simulations with NCEP2-nested RCMs exhibit higher inter-annual variability of mean wind speeds over all regions than is manifest in NARR. The intraannual (month-to-month) variability shows more complex behavior (Figure 6). There is a positive association between inter- and intraannual variability in the RCM simulations. For example, the MM5I simulations within NCEP-2 exhibit both the highest inter- and intraannual variability for the Pacific NW, Midwest, Northeast and the West regions. Equally, lowest inter- and intraannual variability is generally observed in the HadRM3 simulations. This may be partly the result of the extremely low mean wind speeds as simulated by HadRM3 and the resulting suppression of variability in a zero-bounded variable.

[33] The majority of RCM simulations over the Pacific NW exhibit higher intraannual variability ($\sigma_U/\langle U\rangle$ of up to 30%) than is evident in the NARR data set ($\sigma_U/\langle U\rangle \sim 10\%$). Only simulations with HadRM3 nested in both the NCEP-2 and HadCM3 lateral boundary conditions indicate lower intraannual variability in the Pacific NW than is evident in NARR. The NCEP-2/MM5I fields indicate the largest discrepancy with NARR in terms of regional seasonality, while the NCEP-2/CRCM coupling indicates the highest

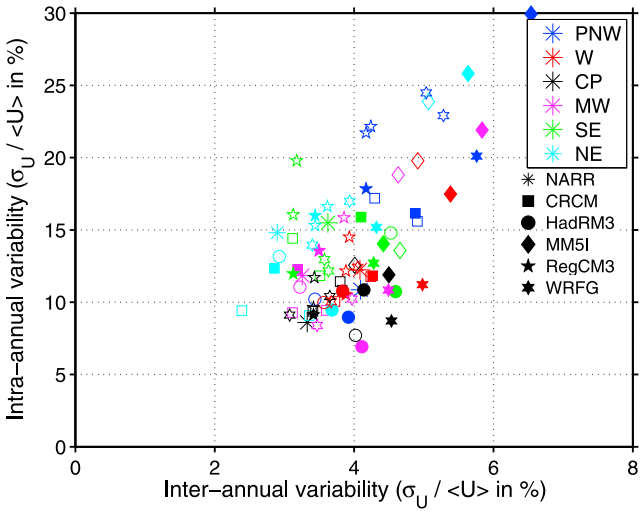

Figure 6. Inter-annual and intraannual variability of mean wind speed (1979–2000) from each of the RCM simulations versus the reference data set (NARR) for each geographic region shown in Figure 2 for 1979–2000. Asterisks denote results from the NARR data set, and the filled symbols for each RCM and region denote simulations in the NCEP-2 lateral boundary conditions. The open symbols denote RCM simulations in the AOGCMs. Note the simulations nested in the AOGCMs are shown by the open symbols, and there are some RCMs that are subject to multiple AOGCM nestings.

degree of agreement. The closest agreement between the seasonality in mean wind speeds from the RCM simulations and NARR is found for the Central Plains and Southeast regions. In the Southeast the NARR data set indicates relatively high intraannual variability of mean wind speeds of approximately 16%, while the RCM simulations nested in NCEP-2 cluster between 11 and 16% and simulations from all RCM-AOGCM combinations lie in the range of 11–20%. NARR indicates the lowest intraannual variability of mean wind speeds in the Central Plains (~8%) and the RCM simulations with lateral boundary conditions from NCEP-2 all lie between 8 and 12%, while results for the AOGCM-RCM combinations fall in the range of 7 to 13%.

[34] At least some of the variations in reproducing the inter-annual variability of wind speeds across the 13 simulations of conditions during 1979–2000 (Figure 6) may be a product of differences in the storm climates as simulated by the models used to provide the RCM lateral boundary conditions. Particularly for the two western regions the inter-annual variability for simulations nested in NCEP-2 exceed that from the AOGCMs. Although the CMIP-3 generation of AOGCMs exhibit similar climatologies to those manifest in NCEP-2 in terms of midlatitude storm tracks and numbers there are subtle differences in those track and particularly the frequency of intense cyclones [*Ulbrich et al.*, 2008].

[35] Consistent with the inference that the NARR data set tends to under-represent regional variations in wind climates, and specifically the higher wind speeds in the Central Plains (cf. Figure 2 and Figure 3b), there is no association between extreme values (U_{50}) derived from the NARR data set and the station observations (Pearson r = 0.01, Spearman r = −0.13) (Figure 7). We place greater emphasis on the Spearman rank correlation coefficients (i.e., the association between two sets of ranked values) because this metric is not based upon an assumption of normality and is less sensitive to outliers such as the single very high U_{50} estimate derived from the NIST data set (Figure 7).

[36] Although the RCM derived extreme wind speeds are biased low relative to estimates derived from the observational records (the negative bias in the spatially averaged extreme wind speeds from the RCM relative to the station estimates is ~8 m s^{-1}), extrapolation of the RCM output to

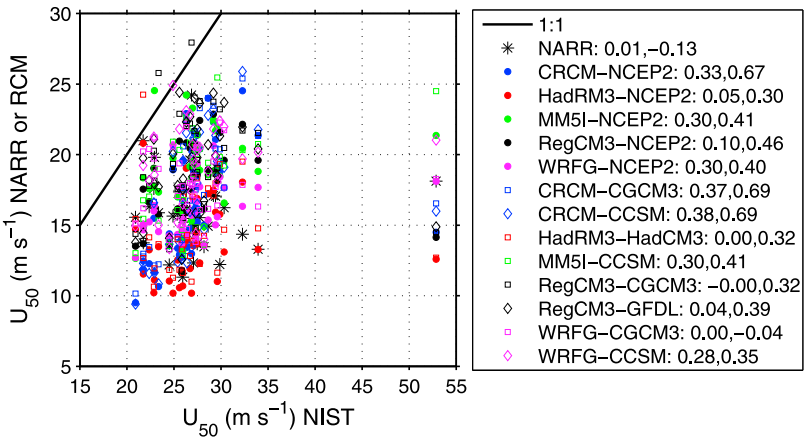

Figure 7. Scatterplot of 50-year return period wind speed at 10-m (computed using equation (1)) based on output from the NARCCAP RCMs in 1979–2000 and from station observations obtained from the National Institute of Standards and Technology (NIST) (see Figure 1 for a map of the station locations). The comparison is for station specific extreme wind speeds and for the grid cells containing those stations. The observed fastest mile wind speeds were transformed into 10-min sustained wind speeds using scaling factors from *Simiu and Scanlan* [1978]. The station data for the fastest mile wind speeds were obtained from the NIST WWW site; www.itl.nist.gov/div898/winds/daily.htm. The numbers shown in the legend depict the Pearson and then Spearman correlation coefficients between the RCM or NARR derived extreme values versus the station derived values.

Table 1. Fraction of Grid Cells (Expressed in Percent) in Each RCM Simulation (on Its Native Grid) That Exhibits the Same Wind Power Class in the 1979–2000 Period Simulations as Manifest in the NREL Wind Resource Assessment[a]

	Lateral Boundary Conditions: AOGCM				
RCM	NCEP-2	CGCM3	CCSM	GFDL	HadCM3
CRCM	14 (57%)	12 (49%)	12 (49%)		
HadRM3	16 (91%)				16 (88%)
MM5I	13 (88%)		17 (84%)		
RegCM3	30 (68%)	29 (59%)		29 (59%)	
WRFG	9 (93%)	18 (70%)	18 (69%)		
NARR	9 (96%)				

[a]*Elliott et al.* [1986]. The classes used and the NREL estimates for wind power class are as shown in Figure 2. The energy density was computed using $E = 0.5\rho U^3$ where the wind speed time series of U had been multiplied by 1.258 to scale from 10-m to 50-m a.g.l. The first number cited is the fraction of grid cell E values from the RCM simulations and NARR that exhibit the same class as those from the NREL resource assessment (wind power classes 2–7). The number in parentheses indicates the fraction of the incorrect WP class estimates that exhibit lower values in the RCM estimates than the NREL assessment. The statistics were computed only for RCM data points where the grid cell centroid is within 19 km of a centroid in the NREL assessment.

derive U_{50} exhibits some skill in manifesting the macroscale variability evident in extreme wind speeds across the contiguous USA (Figure 7; see Figure 2 for location of the stations from which the 50-year return period values derive). The negative bias is consistent with prior research in northern Europe that found increased extreme wind speeds with higher RCM resolution (the fifty-year return period wind speed at 10-m increased by ~24% as the model resolution increased from 50 × 50 km to 6 × 6 km), and that simulations at the higher resolution more closely approximated extreme wind speeds derived from in situ observations away from topographically complex locations [*Pryor et al.*, 2012b].

[37] While CRCM generates spatial fields of the various descriptors of the wind climate that exhibit least agreement with NARR for the lower moments of the wind speed probability distribution (Figure 5), estimates of U_{50} derived from in situ observations indicates relatively good agreement for CRCM nested within both NCEP-2 and the AOGCMs. As shown in Figure 7, both the Pearson and Spearman correlation coefficients between grid-cell average U_{50} from the RCM and estimates from in situ observations is highest for CRCM simulations in all three sets of lateral boundary conditions. However, there is also comparatively high degree of agreement for the MM5I and WRFG simulations conducted within the NCEP-2 lateral boundary conditions (i.e., Pearson (parametric) correlation coefficients ≥ 0.3, and Spearman (nonparametric) correlation coefficients ≥ 0.4). These RCMs (CRCM, MM5I and WRFG) do not use a hydrostatic formulation and might, therefore, be better able to simulate at least some of the dynamics associated with extreme near-surface wind speeds.

[38] Simulations with WRFG nested in NCEP-2 and CCSM generate extreme wind climates that exhibit a relatively high degree of association with the observationally derived extreme wind fields, but extreme values from the WRFG-CGCM3 coupling do not (Figure 7). This is contrary to results from the other two RCMs that were nested in CGCM3 – CRCM and RegCM3, and the source of the discrepancy apparent in the extreme value estimates derived from the WRFG-CGCM3 coupling remains unresolved.

[39] To provide a second independent evaluation of the NARCCAP output, each of the RCM simulations of 1979–2000 were used to compute an average energy density in each grid cell which was scaled to 50 m as described in section 2 and compared to the grid cell categorical estimates from the NREL assessment (shown in Figure 2). It should be acknowledged that applying a single coefficient to scale the RCM output to 50-m neglects the spatial variability in vertical wind shear (and thus the role of phenomena such as low-level jets [*Rife et al.*, 2010]). However, it is consistent with the manner in which the NREL assessment was conducted. The fraction of grid cells for which the RCM output showed the same 'class' of wind resource as that manifest in the NREL estimate, ranges from 9% for the NARR data set to 30% in simulations from NCEP-2/RegCM3 (Table 1). Given that the energy density scales with the cube of the wind speed, it is strongly influenced by the higher percentiles of the wind speed distribution. In addition to examining the degree of fit between the energy density classes, we also report the fraction of grid cells for which the RCM estimate differed from the NREL class. Only simulations from RegCM3 and CRCM exhibit approximately equal fraction of higher and lower estimates than NREL (Table 1). All other data sets – most notably NARR – exhibit substantial negative bias. This finding adds credence to inferences drawn above that CRCM better simulates the upper portion of the wind speed probability distribution than the central tendency, and that there is a negative bias in intense wind speeds as manifest in the NARR. Since only limited evaluation of the 10-m wind speeds from the NARR data set has been conducted, and has focused largely on the lower moments of the distribution [*Kanamaru and Kanamitsu*, 2007; *Mesinger et al.*, 2006; *Pryor et al.*, 2009], the lack of correspondence with station observations derived U_{50} and the energy density values may indicate that the NARR data set may not represent all features of the wind climate with absolute fidelity. One possible source of inaccuracies in the NARR representation of the wind fields is interpolation of the output from native E-grid of the NARR model to a Northern Lambert Conformal Conic projection before the data are archived (see discussion at http://www.atmos.albany.edu/facstaff/rmctc/narr/). This reaffirms the need for further investment in developing robust wind speed climatologies for use in multiple aspects of climate change research including, but not limited to; model evaluation such as that conducted here, and detection and attribution analyses.

3.2. Sensitivity of Simulated Wind Climates to Lateral Boundary Conditions Versus RCM Architecture

[40] Brier skill scores for RCM simulations nested in the AOGCMs are uniformly lower than when NCEP-2 was used as the lateral boundary conditions (Figure 5a). However,

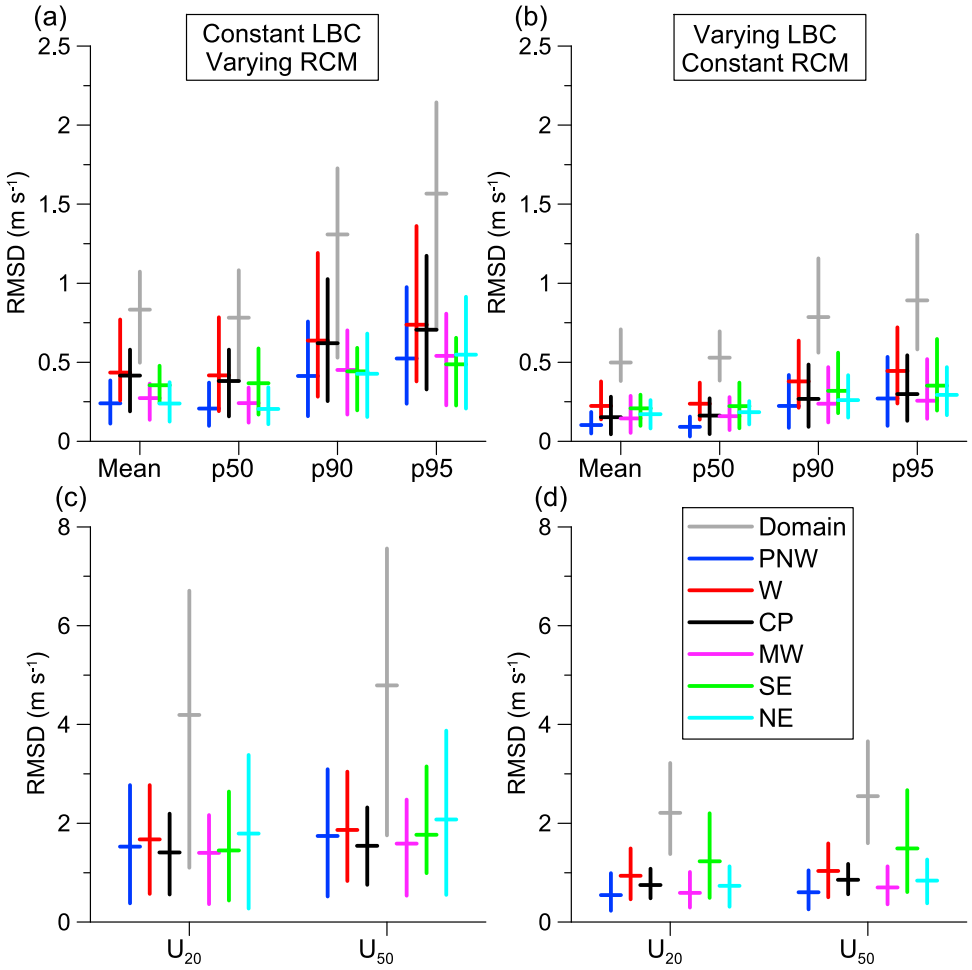

Figure 8. Root mean squared difference (RMSD) between spatial fields of the specified metrics for (a and c) simulations conducted with different RCM nested within the same lateral boundary conditions, and (b and d) for simulations conducted with the same RCM but varying the lateral boundary conditions. Thus, there are results from 10 simulation pairings given in Figures 8a and 8c and eight simulation parings in Figures 8b and 8d. In each case the vertical bars indicate the upper and lower bounds of the RMSD and the horizontal bar shows the arithmetic mean RMSD calculated from the eight or ten AOGCM-RCM pairings. The RMSD for each simulation pairing is computed for the entire study domain and for each of the sub-regions shown in Figure 2.

the RMSD between pairs of RCM simulations with a common RCM but varying lateral boundary conditions are smaller than those computed for common lateral boundary conditions and varying RCM (Figure 8). This finding is true for metrics of the central tendency, intense wind speeds and extreme wind speeds. Thus, at least when aggregated to the regional level, it appears that the wind climate is relatively insensitive to the specific lateral boundary conditions used compared to either the influence of the specific RCM applied, or the magnitude of discrepancies with fields from NARR (Figure 4). For example, the RMSD computed by comparing the spatial fields of 90th percentile wind speeds from a given RCM nested in each AOGCM relative to the field deriving from the same RCM nested in NCEP-2 ranges from 0.56 to 1.16 ms^{-1}. The range of RMSD is smaller than that comparing the five simulations from RCM nested in NCEP-2 (RMSD = 0.53 to 1.73 ms^{-1}), or comparison of the NCEP-2 nested RCM simulations relative to NARR (RMSD = 1.75 to 1.98 ms^{-1}). This is true irrespective of whether the RMSD is computed over the entire study domain or sub-regions thereof (Figure 8).

[41] RCM simulations in the NCEP-2 lateral boundary conditions generally do not indicate a uniform tendency toward greater or lesser accord with the regionally averaged inter- and intraannual variability computed from the NARR data set than do the simulations nested within the AOGCMs (Figure 6). Results shown in Figure 6 and Figure 8b imply that, for the North American study domain, either (i) the AOGCMs are generating similar storm climates (both to each other and NCEP-2) [*Ulbrich et al.*, 2008] and/or (ii) the RCMs are generating conditions associated with wind climates that are to some degree independent of the driving lateral boundary conditions. Note that all AOGCM-RCM simulations exhibit higher average values for all metrics than characterize RCM simulations conducted with lateral boundary conditions supplied by NCEP-2 (Figure 5b). This implies that the RCM simulations are not independent of the lateral boundary conditions, and that the AOGCMs are generating a more

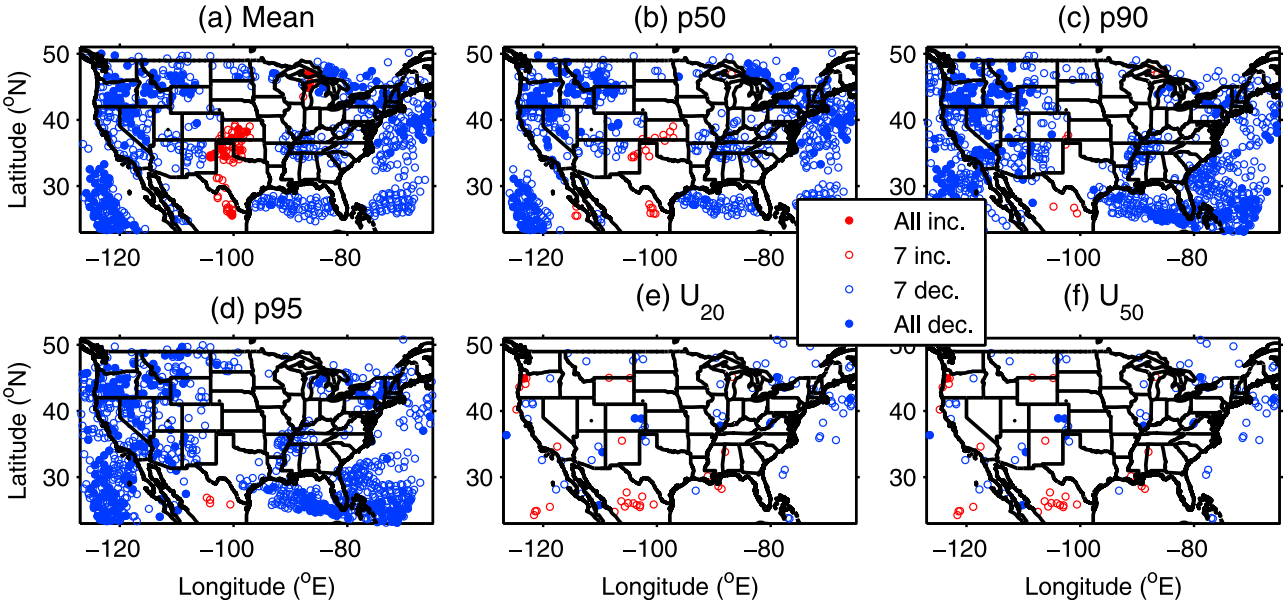

Figure 9. Consistency of the sign of the climate change signal as determined by the number of the RCM simulations that exhibit higher (or lower) values for (a) Mean, (b) 50th percentile, (c) 90th percentile, (d) 95th percentile, (e) 20-year return period and (f) 50-year return period wind speed in 2041–2062 versus 1979–2000. The statistics were computed only for data points where the grid cell centroid for all RCMs is within 19 km of a centroid in NARR. The solid symbols indicate all eight RCM simulations exhibited higher (lower) values in the future period, while the open circles indicate that seven of the eight simulations exhibited higher (lower) values in 2041–2062. Note that the symbols do not depict that magnitude of difference (2041–2062 versus 1979–2000), rather the symbols indicate the number of model simulations that show a difference of a given sign (positive or negative).

active storm climate than is manifest in NCEP-2. For CCSM this is consistent with prior analyses that have indicated that CAM3 (the atmospheric portion of CCSM) exhibits positive bias in wind speeds off the west coast of the USA relative to QuickScat [*Capps and Zender*, 2008]. Nevertheless, for all metrics and all regions, the mean RMSD between spatial fields from the different RCMs exceeds that deriving from variations in the lateral boundary conditions (cf. Figures 8a and 8b). The role of the RCM in causing variations in the spatial fields of intense wind speeds (the 90th and 95th percentile values) appears to be most marked in the West and Central Plains and for entire study domain (Figure 8a). The latter finding appears to result from large discrepancies in high wind speed, offshore areas (Figure 3). The impact of variations in both the RCM and lateral boundary conditions are more marked for the extreme values (Figures 8c and 8d). However, with the exception of the Southeast region, the RCM architecture appears to exhibit a more profound influence on extreme wind speeds than the lateral boundary conditions. One reason why this may not be true for the Southeast, is that the driving AOGCM (or NCEP-2) are playing a critical role in the development and tracking of tropical cyclones which are responsible for the majority of extreme wind events.

[42] The CRCM is subject to spectral nudging throughout the domain, but while there is a slight tendency toward higher average extreme wind speeds from CRCM nested in either CCSM or CGCM3, this tendency is much lower that the statistical uncertainty on the U_{50} and U_{20} estimates due to extrapolation from the annual maxima (see description in *Pryor et al.* [2012a]), and is smaller than variations in extreme wind climates developed from the different RCMs (Figure 8).

3.3. Climate Change Signal

[43] Averaging model output (with or without weighting factors) to generate ensemble projections presents significant challenges, particularly in cases where the number of model simulations is small (such as in this analysis where n = 8) [*Knutti et al.*, 2010]. In this analysis we first examined whether there was coherence in the sign of difference for the mean, 50th percentile, 90th percentile, 95th percentile, and 20 and 50 year return period wind speeds. Spatial fields of a given wind speed metric computed for 2041–2062 were compared with those from 1979 to 2000. Using the criterion that seven of the eight AOGCM-RCM couplings must indicate the same sign of difference between the future (2041–2062) and historical period (1979–2000) as a threshold to identify coherence, this analysis indicates only weak consistency in the climate change signal in any of the descriptors of the wind speed distribution. Almost 18% of grid cells exhibit a lower mean wind speed in all eight of the RCM simulations of the future period relative to the past. It may be worthy of note that the grid-cells that generally indicate increased mean wind speeds are in the region of highest wind energy penetration – in and around northern Texas (Figure 9a). There is greater consistency in terms of the sign of differences between 2041 and 2062 and 1979–2000 for the 90th and 95th percentile wind speeds. Approximately 22% of grid cells exhibit a lower 90th percentile wind speed in all of the RCM simulations (Figure 9c). Although many of

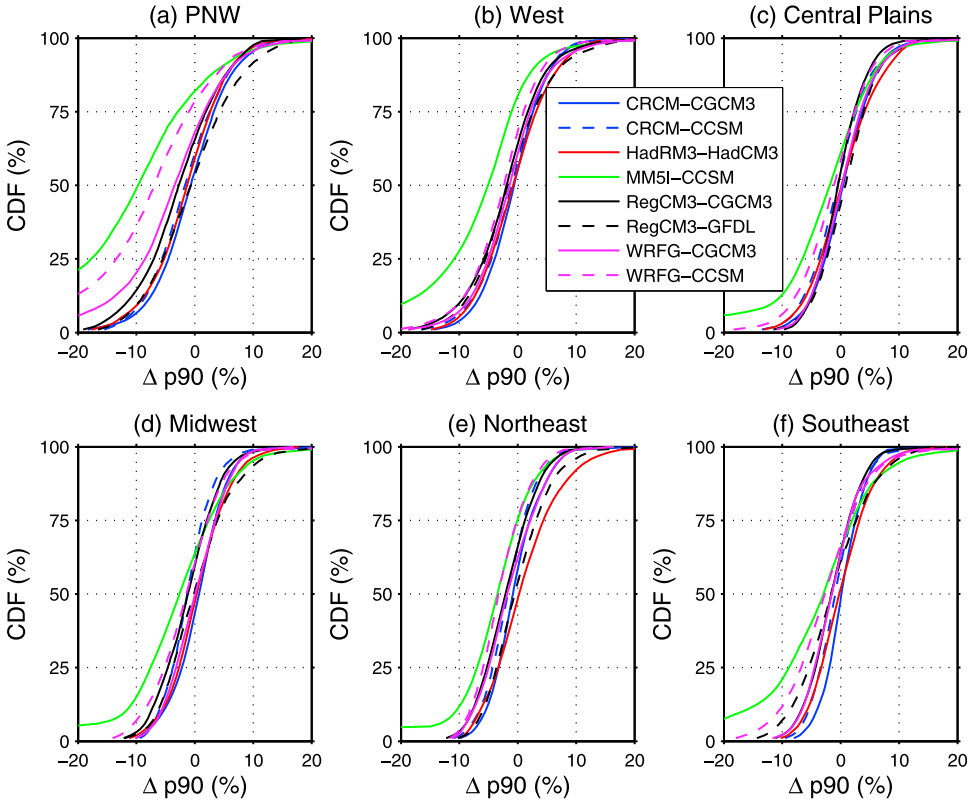

Figure 10. Cumulative probability density functions for the difference in the 90th percentile wind speed; 2041–2062 versus 1979–2000 in each of the six regions (a) Pacific Northwest, (b) West, (c) Central Plains, (d) Midwest, (e) Northeast and (f) Southeast for each of the AOGCM-RCM combinations. The CDF are computed from the spatial fields and thus show the fraction of the grid cells in a given sub-region that exhibits a difference in p90 that has a value less than or equal to that shown on the abscissa.

the grid cells that exhibit a coherent signal of lower intense wind speeds in the future period, are located offshore (e.g., in the Caribbean and off both the southwest and southeast of the USA), where the impact on infrastructure may be comparatively modest. Only 1% of grid cells indicate a consistent signal of either higher or lower values of either the 20- or 50-year return period wind speed in the future period (Figures 9e and 9f). This is consistent with the findings articulated above, that the RCMs are generally developing wind climates that are to some degree independent of the lateral boundary conditions, and that this is particularly true for extreme wind speeds from the non-hydrostatic models.

[44] Spatial cumulative density functions (CDF) for the various wind speed metrics in each region were also compared for the historical and future periods. In accord with expectations, while the evaluation of the RCM derived wind climates during the historical period generally indicate that the skill is determined largely by the choice of RCM, the CDF for projected changes in the 90th percentile wind speeds across the contiguous USA indicate differences in the future relative to the past are determined predominantly by the nesting AOGCM (Figure 10).

[45] RegCM3 simulations in either CGCM3 or GFDL indicate only rather modest changes in the spatial cumulative density function (CDF) of 90th percentile wind speeds in each region in the future versus historical period. Conversely, the MM5I-CCSM simulations indicate largest magnitude differences in the CFD and the highest frequency of reduced wind speeds in all regions (Figure 10). Consistent with the importance of the AOGCMs in dictating the climate change response in storm climates, this tendency toward lower 90th percentile wind speeds in all regions (in 2041–2062 versus 1979–2000) is also observed (though is much less marked) in simulations with WRFG and CRCM nested within CCSM. Conversely, all three RCM simulations (CRCM, RegCM3 and WRFG) within CGCM3 exhibit lower magnitude changes in the spatial CDF and a greater frequency of higher 90th percentile wind speeds in the future period.

[46] The GFDL AOGCM has been shown to exhibit a poleward shift in the major Northern Hemisphere Pacific storm track under warming scenarios [*Wu et al.*, 2011]. Consistent with that tendency, the RegCM3-GFDL simulations indicate modest magnitude increases in 90th percentile wind speeds in the Pacific Northwest. Conversely, simulations with MM5I nested in CCSM indicate that over 75% of grid cells in the West and Pacific Northwest regions exhibit lower values of the 90th percentile wind speed in the future period (Figure 10). The other RCM-AOGCM combinations exhibit almost equal numbers of grid cells with declining and increasing values in most of the regions. With the exception of the WRFG and MM5I simulations for the Pacific Northwest and the MM5I simulations for the other regions, >99% of grid cells in any region exhibit differences of less than ±20% relative to the historical period (Figure 10). Similar results

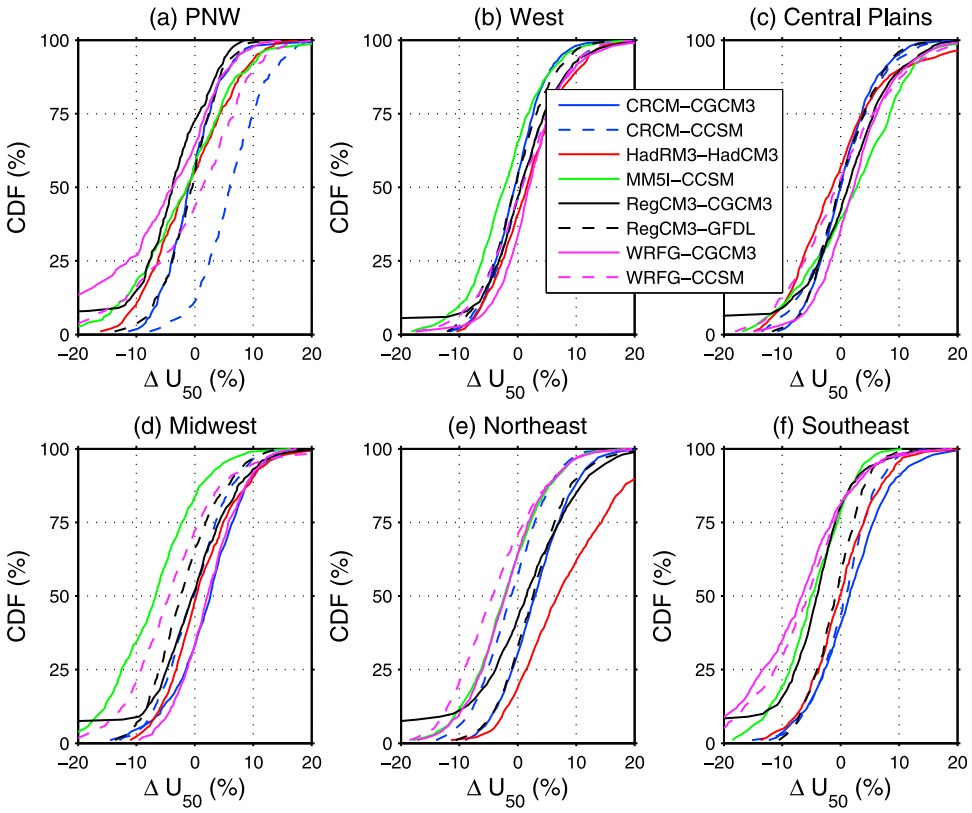

Figure 11. Cumulative probability density functions for the difference in the 50-year return period wind speed; 2041–2062 versus 1979–2000 in each of the six regions (a) Pacific Northwest, (b) West, (c) Central Plains, (d) Midwest, (e) Northeast and (f) Southeast for each of the AOGCM-RCM combinations. The CDF are computed from the spatial fields and thus show the fraction of the grid cells in a given sub-region that exhibits a difference in U_{50} that has a value less than or equal to that shown on the abscissa.

were found for the two measures of central tendency (mean and 50th percentile wind speed), although the fractional changes in the central tendency are generally smaller than those in the 90th percentile values.

[47] The spatial CDF for differences in the 50-year return period wind speed exhibit greater divergence between the eight sets of simulations. There is some weak evidence for consistency in the magnitude and dominant change of sign in simulations with differing RCM nested in the same AOGCM. All three of the CGCM3 nested simulations indicate increased U_{50} over parts of the Central Plains (Figure 11c). Nevertheless, the climate change signal is not uniform across all AOGCM-RCM couplings in a given region or across regions. The HadRM3-HadCM3 simulation indicates over 80% of grid cells in the Northeast will exhibit increased extreme wind speeds in contrast with WRFG-CCSM and WRFG-CGCM3 simulations that indicate up to two-thirds of grid cells will exhibit decreased values in the future (Figure 11e). Additionally while the extreme values derived from simulations with MM5I and WRFG in CCSM generally indicate a dominance of lower values in the future period over the Midwest (Figure 11d), the CRCM-CCSM simulations indicate almost equal fraction of grid cells with higher and lower values. This indicates that the RCM is also mediating the climate change signal. For example, CRCM in both CCSM and CGCM3 indicate a tendency toward increased extreme wind speeds in the Southeast (Figure 11f).

[48] There is no evidence that the weaker climate change response of CCSM with respect to temperatures is associated with an amplification or suppression of the difference in wind regimes over the contiguous USA in the future period relative to 1979–2000.

[49] Consistent with differences in the mechanisms responsible for dictating the extreme and 90th percentile wind speed values, projected changes in the regional CDFs for 90th percentile and 50-year return period wind speeds indicate some evidence for divergent trajectories in these two metrics from individual RCMs. For example, output from the HadCM3-HadRM3 coupling indicates approximately equal areas with increased and decreased 90th percentile wind speeds in the Northeast (Figure 10e) while over three-quarters of the Northeast region exhibit higher extreme wind speeds in the future period (Figure 11e).

[50] The ranges of projected differences in 90th percentile and 50-year return period wind speeds expressed in Figures 10 and 11 are not representative of the full range of plausible differences in wind climates in 2041–2062 versus 1979–2000. It is likely that these simulations under-sample the true uncertainty space. In keeping with the prior analyses summarized in section 1, the results tend to imply that while this suite of RCM simulations indicates some consistency in projecting declines in the 90th percentile wind speed

particularly in the western USA, those tendencies are likely to be of comparatively modest magnitude and to exhibit sub-regional variability in sign and magnitude (Figure 10). It is also important to note that the wind climate exhibits large inherent variability at a range of time scales from minutes to decades. Analyses of a single future time period of only 22 years duration precludes extrapolation to infer possible trends in any aspect of the wind climate, only differences in two temporal windows.

4. Concluding Remarks

[51] A key question in regional downscaling of climate information may be phrased as 'does higher resolution modeling add value when compared to global model results?' To determine whether the dynamical downscaling undertaken within NARCCAP leads to greater validity of output fields of wind climate descriptors, the RCM output was evaluated relative to NARR and the wind climate as simulated in the NCEP-2 reanalysis which was used to provide lateral boundary conditions. Wind climates as simulated by the five RCMs nested in the NCEP-2 reanalysis along with output from the NCEP-2 reanalysis itself and station data exhibit greater spatial variability than is manifest in the NARR data set. All RCM simulations nested in NCEP-2 outperform those from AOGCM-RCM couplings when NARR is used as the target. No RCM exhibits uniformly 'best' performance relative to NARR for all similarity metrics (RMSD, correlation coefficients, bias, and ratio of spatial variability) and all wind speed distribution descriptors (mean, median, 90th and 95th percentiles and 20 and 50 year return period wind speeds) (Figure 5). Using the NARR data set as the 'target' and NCEP-2 reanalysis as the reference forecast it is demonstrated that application of the RCMs almost uniformly 'adds value' to depiction of the wind climate over the contiguous USA. That implies that when the RCMs are applied in type 2 dynamical downscaling contexts (wherein the RCM is nested in reanalysis data *Castro et al.* [2005]), perhaps by virtue of the more detailed description of surface boundary forcing, they generate more realistic atmospheric variability at the meso/synoptic scale. The BSS for simulations conducted in type 4 dynamical downscaling (where the lateral boundary conditions are supplied from AOGCM *Castro et al.* [2005]) also exhibit some evidence for value-added in simulation of extreme wind speeds across the contiguous USA.

[52] With the exception of the NCEP-2/HadRM3 simulations all 12 other RCM-AOGCM couplings exhibit a positive mean bias relative to NARR for all six of the descriptors of the wind climate during 1979–2000. Estimated over all six descriptors of the wind speed probability distribution and all performance metrics NCEP-2/WRFG simulations exhibit highest agreement with respect to the NARR data set, although NCEP-2/WRFG performs less well for the extreme wind speeds (Figure 5).

[53] There is a positive association between inter- and intraannual variability in the RCM simulations of the 1979–2000 period, and some evidence that RCMs that exhibit high intra and inter-annual variability in the historical period may be more likely to exhibit a stronger climate change signal. For example, MM5I simulations in the historical period exhibit high inter- and intraannual variability across all regions of the contiguous USA and both sets of lateral boundary conditions (NCEP-2 and CCSM) (Figure 6). Simulations for the CCSM-MM5I coupling also exhibit some evidence for a particularly strong climate change signal (i.e., larger difference in the 2041–2062 versus 1979–2000 periods) (Figure 10).

[54] Analysis of output from the non-hydrostatic models does not appear to demonstrate clear 'improvement' in characterization of the wind climate as manifest in NARR. However, output from CRCM does perform 'best' relative to extreme values in situ observations (Figure 7). This may imply that a non-hydrostatic formulation and/or the spectral nudging applied to the CRCM throughout the domain improves the simulation of extreme wind speeds even when the RCM is applied at 50 km resolution.

[55] Based on analyses presented herein it appears that the RCMs employed generate wind climates at a nominal height of 10-m across the contiguous USA that are, to some degree, independent of the lateral boundary conditions. Although Brier Skill Scores for simulations wherein the RCM is nested in AOGCM output indicate lower agreement with NARR than simulations conducted within NCEP-2, the RMSD between fields of the wind climates for the entire study domain and sub-regions thereof show higher values for variations between RCM than for simulations within a single RCM nested in a variety of lateral boundary conditions (Figures 5 and 8). Indeed the mean RMSD between spatial fields of each of the wind speed metrics is almost twice as large for variations in the RCM applied as for variations in the lateral boundary conditions.

[56] Wind climates from eight RCM simulations for the middle-twenty-first century (2041–2062) are compared to those for the historical period (1979–2000). The results indicate some evidence for lower values of the central tendency and the 90th and 95th percentile wind speeds in the future period, but the degree of agreement in the sign of the climate change signal between the simulations is relatively low. No change is observed in the extreme wind speeds.

[57] Returning to the questions that motivated this research, the primary findings of these analyses indicate:

[58] 1. The NARCCAP RCM suite exhibits clear 'value added' in depicting wind climates across the contiguous USA relative to NCEP-2. The degree of skill in reproducing the contemporary wind climate as manifest in NARR varies considerably with wind speed metric for a given AOGCM-RCM coupling. No AOGCM-RCM coupling exhibits uniformly 'best' performance relative to NARR, station-based extreme wind speed estimates or the NREL grid wind power classes. Given this, it would appear prudent to consider the full suite of model combinations for impact analyses, although there appears to be some justification for use of the non-hydrostatic models for extreme wind speeds.

[59] 2. Simulations of the contemporary wind climate exhibit greater variations with the RCM than due to variations in the lateral boundary conditions. However, generally RCM simulations nested in NCEP-2 exhibit greater accord with NARR, station-based extreme wind speed estimates or the NREL grid wind power classes.

[60] 3. Comparing various metrics of the wind climates as simulated for 2041–2062 with those from 1979 to 200 indicates some evidence for lower values of the central

tendency and the 90th and 95th percentile wind speeds in the future period, particularly in the western USA. However, all eight of the AOGCM-RCM combinations exhibit at least some grid-cells with higher, central tendency, intense and extreme winds in all six study regions. There is also some evidence that AOGCM-RCM combinations that exhibit high inter- and intraannual variability in the 1979–2000 period exhibit the largest magnitude changes in wind regimes.

[61] **Acknowledgments.** Financial support was supplied by the National Science Foundation (grants 1019603 and 1067007). We wish to thank the North American Regional Climate Change Assessment Program (NARCCAP) for providing the RCM output used in this paper. NARCCAP is funded by the National Science Foundation (NSF), the U.S. Department of Energy (DoE), the National Oceanic and Atmospheric Administration (NOAA), and the U.S. Environmental Protection Agency Office of Research and Development (EPA). The NREL wind power resource estimates were kindly provided by Dennis Elliott. The authors gratefully acknowledge helpful suggestions made by two reviewers.

References

Abild, J., E. Y. Andersen, and D. Rosbjerg (1992), The climate of extreme winds at the Great Belt, Denmark, *J. Wind Eng. Industrial Aerodyn.*, *41*(1–3), 521–532.

Angeles, M. E., J. E. Gonzalez, D. J. Erickson III, and J. L. Hernandez (2010), The impacts of climate changes on the renewable energy resources in the Caribbean region, *J. Sol. Energy Eng.*, *132*(3), 031009, doi:10.1115/1.4001475.

Banik, S. S., H. P. Hong, and G. A. Kopp (2010), Assessment of capacity curves for transmission line towers under wind loading, *Wind Struct.*, *13*(1), 1–20.

Bärring, L., and K. Fortuniak (2009), Multi-indices analysis of southern Scandinavian storminess 1780–2005 and links to interdecadal variations in the NW Europe–North Sea region, *Int. J. Climatol.*, *29*, 373–384, doi:10.1002/joc.1842.

Breslow, P. B., and D. J. Sailor (2002), Vulnerability of wind power resources to climate change in the continental United States, *Renew. Energy*, *27*, 585–598, doi:10.1016/S0960-1481(01)00110-0.

Capps, S. B., and C. S. Zender (2008), Observed and CAM3 GCM sea surface wind speed distributions: Characterization, comparison, and bias reduction, *J. Clim.*, *21*(24), 6569–6585, doi:10.1175/2008JCLI2374.1.

Castro, C. L., R. A. Pielke, and G. Leoncini (2005), Dynamical downscaling: Assessment of value retained and added using the regional atmospheric modeling system (RAMS), *J. Geophys. Res.*, *110*, D05108, doi:10.1029/2004JD004721.

Chang, E. K. M., S. Y. Lee, and K. L. Swanson (2002), Storm track dynamics, *J. Clim.*, *15*(16), 2163–2183, doi:10.1175/1520-0442(2002)015<02163:STD>2.0.CO;2.

Collins, W. D., et al. (2006), The Community Climate System Model version 3(CCSM3), *J. Clim.*, *19*(11), 2122–2143, doi:10.1175/JCLI3761.1.

Cook, N. J. (1986), *The Designer's Guide to Wind Loading of Building Structures: Part 1: Background, Damage Survey, Wind Data and Structural Classification*, 383 pp., Butterworth, London.

Delworth, T. L., et al. (2006), GFDL's CM2 global coupled climate models - Part 1: Formulation and simulation characteristics, *J. Clim.*, *19*, 643–674, doi:10.1175/JCLI3629.1.

Elía, R., and H. Côté (2010), Climate and climate change sensitivity to model configuration in the Canadian RCM over North America, *Meteorol. Z.*, *19*(4), 325–339, doi:10.1127/0941-2948/2010/0469.

Elliott, D. L., C. G. Holladay, W. R. Barchet, H. P. Foote, and W. F. Sandusky (1986), *Wind Energy Resource Atlas of the United States*, 210 pp., Sol. Tech. Inf. Program, U.S. Dep. of Energy, Washington, D. C.

Feser, F., B. Rockel, H. von Storch, J. Winterfeldt, and M. Zahn (2011), Regional climate models add value to global model data: A review and selected examples, *Bull. Am. Meteorol. Soc.*, *92*(9), 1181–1192, doi:10.1175/2011BAMS3061.1.

Garratt, J. R. (1992), *The Atmospheric Boundary Layer*, Cambridge Univ. Press, Cambridge, U. K.

Grell, G. A., J. Dudhia, and D. R. Stauffer (1995), A description of the Fifth-Generation Penn State/NCAR Mesoscale Model (MM5), report, Natl. Cent. for Atmos. Res., Boulder, Colo.

Hawkins, E., and R. Sutton (2009), The potential to narrow uncertainty in regional climate projections, *Bull. Am. Meteorol. Soc.*, *90*(8), 1095–1107, doi:10.1175/2009BAMS2607.1.

Held, I. M. (1993), Large-scale dynamics and global warming, *Bull. Am. Meteorol. Soc.*, *74*(2), 228–241, doi:10.1175/1520-0477(1993)074<0228:LSDAGW>2.0.CO;2.

Intergovernmental Panel on Climate Change (2007), *Climate Change 2007: The Physical Science Basis. Contribution of Working Group I to the Fourth Assessment Report of the Intergovernmental Panel on Climate Change*, edited by S. Solomon et al., 996 pp., Cambridge Univ. Press, Cambridge, U. K.

Jones, R. G., M. Noguer, D. C. Hassell, D. Hudson, S. S. Wilson, G. J. Jenkins, and J. F. B. Mitchell (2004), Generating high resolution climate change scenarios using PRECIS, report, 35 pp., Met Office Hadley Cent., Exeter, U. K.

Kanamaru, H., and M. Kanamitsu (2007), Fifty-seven-year California Reanalysis Downscaling at 10 km (CaRD10). Part II: Comparison with North American Regional Reanalysis, *J. Clim.*, *20*(22), 5572–5592, doi:10.1175/2007JCLI1522.1.

Kanamitsu, M., W. Ebisuzaki, J. Woollen, S. K. Yang, J. J. Hnilo, M. Fiorino, and G. L. Potter (2002), NCEP-DOE AMIP-II reanalysis (R-2), *Bull. Am. Meteorol. Soc.*, *83*(11), 1631–1643, doi:10.1175/BAMS-83-11-1631.

Kay, A. L., H. N. Davies, V. A. Bell, and R. G. Jones (2009), Comparison of uncertainty sources for climate change impacts: Flood frequency in England, *Clim. Change*, *92*(1–2), 41–63, doi:10.1007/s10584-008-9471-4.

Knutti, R., R. Furrer, C. Tebaldi, J. Cermak, and G. A. Meehl (2010), Challenges in combining projections from multiple climate models, *J. Clim.*, *23*(10), 2739–2758, doi:10.1175/2009JCLI3361.1.

Kunz, M., S. Mohr, M. Rauthe, R. Lux, and C. Kottmeier (2010), Assessment of extreme wind speeds from Regional Climate Models - Part 1: Estimation of return values and their evaluation, *Nat. Hazards Earth Syst. Sci.*, *10*(4), 907–922, doi:10.5194/nhess-10-907-2010.

Laprise, R. (2003), Resolved scales and nonlinear interactions in limited-area models, *J. Atmos. Sci.*, *60*(5), 768–779, doi:10.1175/1520-0469(2003)060<0768:RSANII>2.0.CO;2.

Lu, X., M. B. McElroy, and J. Kiviluoma (2009), Global potential for wind-generated electricity, *Proc. Natl. Acad. Sci. U. S. A.*, *106*, 10,933–10,938, doi:10.1073/pnas.0904101106.

Mearns, L. O., W. Gutowski, R. Jones, R. Leung, S. McGinnis, A. Nunes, and Y. Qian (2009), A regional climate change assessment program for North America, *Eos Trans. AGU*, *90*(36), 311–312, doi:10.1029/2009EO360002.

Mesinger, F., et al. (2006), North American regional reanalysis, *Bull. Am. Meteorol. Soc.*, *87*(3), 343–360, doi:10.1175/BAMS-87-3-343.

Murphy, A. H., and E. S. Epstein (1989), Skill scores and correlation-coefficients in model verification, *Mon. Weather Rev.*, *117*(3), 572–582, doi:10.1175/1520-0493(1989)117<0572:SSACCI>2.0.CO;2.

Nakicenovic, N., and R. Swart (Eds.) (2000), *Emissions Scenarios 2000*, 570 pp., Cambridge Univ. Press, Cambridge, U. K.

O'Gorman, P. A. (2010), Understanding the varied response of the extratropical storm tracks to climate change, *Proc. Natl. Acad. Sci. U. S. A.*, *107*(45), 19,176–19,180, doi:10.1073/pnas.1011547107.

Pal, J. S., et al. (2007), Regional climate modeling for the developing world - The ICTP RegCM3 and RegCNET, *Bull. Am. Meteorol. Soc.*, *88*, 1395–1409, doi:10.1175/BAMS-88-9-1395.

Pan, L.-L., S.-H. Chen, D. Cayan, M.-Y. Lin, Q. Hart, M.-H. Zhang, Y. Liu, and J. Wang (2011), Influences of climate change on California and Nevada regions revealed by a high-resolution dynamical downscaling study, *Clim. Dyn.*, *37*(9–10), 2005–2020, doi:10.1007/s00382-010-0961-5.

Pope, V., M. Gallani, P. Rowntree, and R. Stratton (2000), The impact of new physical parameterizations in the Hadley Centre climate model: HadAM3, *Clim. Dyn.*, *16*, 123–146, doi:10.1007/s003820050009.

Pryor, S. C., and R. J. Barthelmie (2011), Assessing climate change impacts on the near-term stability of the wind energy resource over the USA, *Proc. Natl. Acad. Sci. U. S. A.*, *108*, 8167–8171, doi:10.1073/pnas.1019388108.

Pryor, S. C., and J. Ledolter (2010), Addendum to "Wind speed trends over the contiguous USA," *J. Geophys. Res.*, *115*, D10103, doi:10.1029/2009JD013281.

Pryor, S. C., and J. T. Schoof (2010), Importance of the SRES in projections of climate change impacts on near-surface wind regimes, *Meteorol. Z.*, *19*(3), 267–274.

Pryor, S. C., R. J. Barthelmie, and E. Kjellström (2005), Analyses of the potential climate change impact on wind energy resources in northern Europe using output from a regional climate model, *Clim. Dyn.*, *25*, 815–835, doi:10.1007/s00382-005-0072-x.

Pryor, S. C., R. J. Barthelmie, D. T. Young, E. S. Takle, R. W. Arritt, D. Flory, W. J. Gutowski, A. Nunes, and J. Roads (2009), Wind speed trends over the contiguous United States, *J. Geophys. Res.*, *114*, D14105, doi:10.1029/2008JD011416.

Pryor, S. C., R. J. Barthelmie, N. E. Clausen, M. Drews, N. MacKellar, and E. Kjellstrom (2012a), Analyses of possible changes in intense and

extreme wind speeds over northern Europe under climate change scenarios, *Clim. Dyn.*, *38*, 189–208, doi:10.1007/s00382-00010-00955-00383.

Pryor, S. C., G. Nikulin, and C. Jones (2012b), Influence of spatial resolution on Regional Climate Model derived wind climates, *J. Geophys. Res.*, *117*, D03117, doi:10.1029/2011JD016822.

Reed, D. A. (2008), Electric utility distribution analysis for extreme winds, *J. Wind Eng. Ind. Aerodyn.*, *96*(1), 123–140, doi:10.1016/j.jweia.2007.04.002.

Rife, D. L., J. O. Pinto, A. J. Monaghan, C. A. Davis, and J. R. Hannan (2010), Global distribution and characteristics of diurnally varying low-level jets, *J. Clim.*, *23*(19), 5041–5064, doi:10.1175/2010JCLI3514.1.

Rowell, D. P. (2006), A demonstration of the uncertainty in projections of UK climate change resulting from regional model formulation, *Clim. Change*, *79*(3–4), 243–257, doi:10.1007/s10584-006-9100-z.

Sailor, D. J., M. Smith, and M. Hart (2008), Climate change implications for wind power resources in the northwest United States, *Renewable Energy*, *33*, 2393–2406, doi:10.1016/j.renene.2008.01.007.

Santer, B. D., et al. (2009), Incorporating model quality information in climate change detection and attribution studies, *Proc. Natl. Acad. Sci. U. S. A.*, *106*(35), 14,778–14,783, doi:10.1073/pnas.0901736106.

Schwierz, C., P. Koellner-Heck, E. Mutter, D. N. Bresch, P. Vidale, M. Wild, and C. Schaer (2010), Modelling European winter wind storm losses in current and future climate, *Clim. Change*, *101*(3–4), 485–514, doi:10.1007/s10584-009-9712-1.

Scinocca, J. F., N. A. McFarlane, M. Lazare, J. Li, and D. Plummer (2008), Technical Note: The CCCma Third Generation AGCM and its extension into the middle atmosphere, *Atmos. Chem. Phys.*, *8*(23), 7055–7074, doi:10.5194/acp-8-7055-2008.

Simiu, E., and R. H. Scanlan (1978), *Wind Effects on Structures: An Introduction to Wind Engineering*, 458 pp., John Wiley, Hoboken, N. J.

Skamarock, W. C., J. B. Klemp, J. Dudhia, D. O. Gill, D. M. Barker, W. Wang, and J. G. Powers (2005), A description of the Advanced Research WRF version 2, report, 88 pp., NCAR, Boulder, Colo.

Ulbrich, U., J. G. Pinto, H. Kupfer, G. C. Leckebusch, T. Spangehl, and M. Reyers (2008), Changing Northern Hemisphere storm tracks in an ensemble of IPCC climate change simulations, *J. Clim.*, *21*(8), 1669–1679, doi:10.1175/2007JCLI1992.1.

von Storch, H., and F. W. Zwiers (1999), *Statistical Analysis in Climate Research*, 494 pp., Cambridge Univ. Press, Cambridge, U. K.

Weisse, R., and H. von Storch (2010), Past and future changes in wind, wave and storm surge climates, in *Marine Climate and Climate Change: Storms, Wind Waves and Storm Surges*, pp. 165–203, Springer Praxis, London.

Weitzman, M. L. (2011), Fat-tailed uncertainty in the economics of catastrophic climate change, *Rev. Environ. Econ. Policy*, *5*(2), 275–292, doi:10.1093/reep/rer006.

Winterfeldt, J., B. Geyer, and R. Weisse (2011), Using QuikSCAT in the added value assessment of dynamically downscaled wind speed, *Int. J. Climatol.*, *31*(7), 1028–1039, doi:10.1002/joc.2105.

Woollings, T. (2010), Dynamical influences on European climate: An uncertain future, *Philos. Trans. R. Soc. A*, *368*(1924), 3733–3756.

Wu, Y., M. Ting, R. Seager, H.-P. Huang, and M. A. Cane (2011), Changes in storm tracks and energy transports in a warmer climate simulated by the GFDL CM2.1 model, *Clim. Dyn.*, *37*(1–2), 53–72, doi:10.1007/s00382-010-0776-4.